JOURNAL OF MATERIALS SCIENCE **34** (1999) 727–733

Nebulized spray deposition of PLT thin film

C. S. HUANG, J. S. CHEN, C. H. LEE
Department of Materials Science & Engineering, Cheng Kung University, Tainan, Taiwan
E-mail: leec@dblab.iie.ncku.edu.tw

Films of lead lanthanum titanate (PLT) are deposited on n-type (100) Si and $Pt/TiO_2/Ti/SiO_2/(100)Si$ substrates by using ultrasonic nebulized spray deposition. In this work, $Pb(CH_3COO)_2 \cdot 3H_2O$, $La(NO_3)_3 \cdot 6H_2O$, $Ti(i\text{-}C_3H_7O)_4$ are used as reactants. Experimental results reveal that the films are transformed from tetragonal to nearly cubic as the lanthanum content increases. The refractive index and grain size decrease with the increase of La content in the films. From C-V and I-V measurements of the Al/PLT/n-Si (MIS) and $Pt/PLT/Pt/TiO_2/Ti/SiO_2/n\text{-}Si$ (MIM) structures, the dielectric properties are determined. The permittivities are found to increase with the La content to a maximum value of about 275 and 530 for the MIS and MIM structures, respectively, and then decrease with further increase of La content for the films grown at 550 °C. The results of I-V measurements indicate that the leakage currents of the MIS structure are higher than in the MIM structure. The P-E hysteresis loop became slimmer with the increase of La concentration due to lower tetragonality (c/a), and when the La content is higher than 20 mol %, the films behave like a normal dielectric.

1. Introduction

In order to increase the density of memory cells in the next generation of DRAMs, there has been a growing interest in perovskite materials due to their high dielectric permittivities (and dielectric strengths). Ferroelectric materials are receiving much attention because they are thought to satisfy most of the requirements for the DRAMs application. However there exist several disadvantages for the use of switching ferroelectric thin films (even if operated in unipolar) [1, 2], such as the occurrence of potential fatigue problem, increase of loss tangent, and the delay of charging and discharging speeds of the capacitors. Therefore, nonswitching cubic paraelectric dielectrics with extremely high permittivity should offer significant advantages over their ferroelectric counterparts for unipolar nonswitching operations in ULSI DRAMs [3]. The preparation techniques of cubic paraelectric perovskite PLT thin films include sputtering [4–9], electron-beam evaporation [10], sol-gel [11–15], laser ablation [16, 17], metal organic decomposition (MOD) [18], and metallorganic chemical vapor deposition (MOCVD) [19–22]. Among these methods, MOCVD is a promising process because of its potential advantages to deposit high-quality thin films on Si wafers for volume production. The success of the MOCVD process depends critically on the volatility and stability of the precursor materials. The metalorganic sources in MOCVD are generally a liquid of high vapor pressure or a solid source heated to a relatively high temperature in order to obtain the proper vapor pressure. For better control of the reaction, the gas lines between the source bottles and the reaction chamber are mostly kept at an elevated temperature to prevent the condensation of the sources. Therefore, the equipment becomes very complex and difficult to maintain. However, in the deposition process of ultrasonic nebulized spray pyrolysis, the raw material sources of low vapor pressure can be used without heating up the gas lines. The equipment requirement becomes simpler and the problems of the source materials' reaction are overcome. The source droplets made by the ultrasonic waves have very small sizes with a narrow size distribution and no inertia in their movement, so that they can be transported by the carrier gases without heating. The solvent vaporizes as the droplets approach the substrate. The reactants diffuse to the substrate and a heterogeneous reaction occurs [23]. In this work, PLT thin films are deposited by using ultrasonic nebulized CVD to yield polycrystalline thin films at relatively low temperature, compatible with integrated circuit (IC) processes. The nature of the process and the effects of La concentration and the film microstructure on electric properties are discussed in this paper.

2. Experiment

The experimental work on ultrasonic nebulized spray pyrolysis for growth of PLT thin films was carried out in a homemade reaction chamber schematically illustrated in Fig. 1. The details of this experimental system were reported elsewhere [24]. In this work, n-type (100) Si wafers and platinum coated silicon were used as substrates. The metallizations with Pt(150 nm)/TiO_2(4 nm)/Ti(4 nm)/SiO_2(100 nm)/Si structure were fabricated by electron beam evaporation as follows: (100) Si wafers were first oxidized in wet oxygen at 950 °C to form SiO_2 barrier layer with thickness about

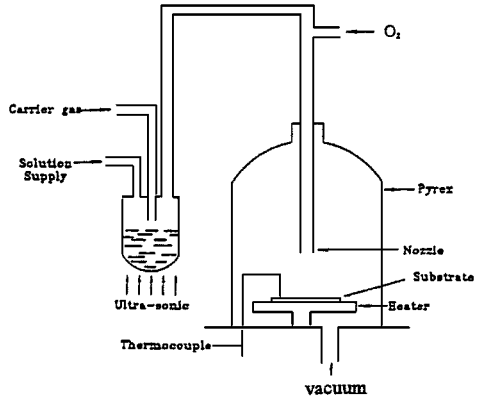

Figure 1 Setup of the spray pyrolysis system.

100 nm. A thin Ti layer was deposited onto the silica to improve adhesion of Pt to the silica. Then a thin TiO_2 layer was deposited on Ti layer before the Pt layer to prevent the diffusion of Ti along the Pt grain boundary.

The precursor solution was prepared as follows: $Pb(CH_3COO)_2{\cdot}3H_2O$ and $La(NO_3)_3{\cdot}6H_2O$ were dissolved at 70 °C in 2-methoxyethanol ($CH_3OCH_2CH_2$-OH, b.p.:124.4 °C), continuously heated at 110 °C for 30 minutes in order to remove the water, and then cooled to room temperature. Titanium isopropoxide, $Ti(i\text{-}C_3H_7O)_4$, was mixed with acetylacetone in the proportion of 1 : 2 before being added into the Pb and La precursor solution. Finally, we added a little acetic acid to keep the solution clear and diluted it with 2-methoxyethanol. The spray solution was nebulized ultrasonically with a spray rate of 1 cc/min. The vapor was introduced into the reaction chamber by means of Ar with O_2 as the carrier gas with a flow rate of 750 sccm. The reaction pressure was fixed at 70 torr. The distance of the nozzle from the substrate was kept at 5 centimeters. The La concentration of the precursor solution was varied from 5 mol % to 35 mol % to investigate its effects on growth rate, refractive index, crystal structure, surface morphology and electric properties in order to optimize the process.

The properties of the thin films in this work were characterized by various standard techniques. Namely, the thickness and refractive index were measured with an α-step meter and an ellipsometer respectively. The crystal structure and composition of the films are analysed by means of X-ray diffraction and XPS (X-ray photoelectron spectroscopy) respectively. The surface morphology of the films is analysed by means of SEM. The I-V and C-V characteristics are measured by means of HP4195B and HP4192A meters respectively. P-E curves are obtained by measurements under an applied voltage of ± 10 V using a RT66A ferroelectric test system from Radiant Technologies.

3. Results and discussion

In order to reduce the experimental variables in this work, the thicknesses of all the films were fixed at about 300 nm. The concentration of the precursor solutions is kept at 0.015 M for $Pb_{1-x/100}La_{x/100}Ti_{1-x/400}O_3$ (PLT(x)), where $x = 5$, 10, 15, 20, 25, 30 and 35. When the La content in the precursor solution is higher than 35 mol % there are excessive particles formed and incorporated into the films, which degrade their quality. In this work, by using the above mentioned precursor solutions, the as-deposited films are always mirror smooth.

3.1. Deposition on n-type (100) Si

Fig. 2 shows that the growth rate depends strongly on the deposition temperature and the La content of precursor solution. It indicates that in the lower temperature range the growth rate increases with temperature because of the increase in reaction rate. The growth rate reaches a maximum at about 550 °C to 590 °C and then decreases with further increase of temperature because of source depletion due to homogeneous reaction. Fig. 2 also indicates that the growth rate decreases with increasing La content in the precursor solution. This is probably due to the chemical reaction which occurs to form an adduct when the $La(NO_3)_3{\cdot}6H_2O$ is added into the precursor solution and the decomposition rate decreases. The film composition varies with growth temperature. It is measured as a function of deposition temperature by means of ESCA. In our previous work on the PZT thin films [24], 550 °C is the optimized deposition temperature to maintain a proper content of Pb in the film. Therefore, in Fig. 3 we use this temperature to investigate the relationship of film composition to

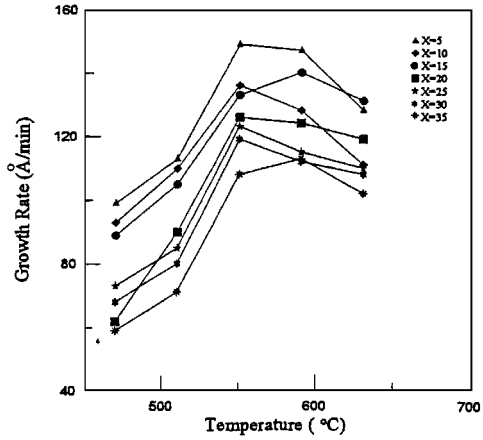

Figure 2 Dependence of growth rate on growth temperature with various La content of precursor solution.

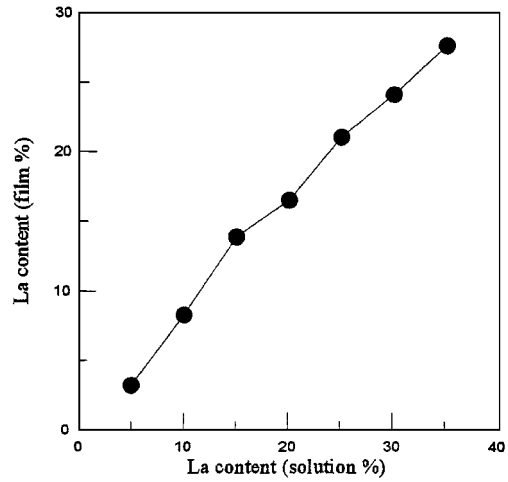

Figure 3 Dependence of film composition on precursor composition for films deposited at 550 °C.

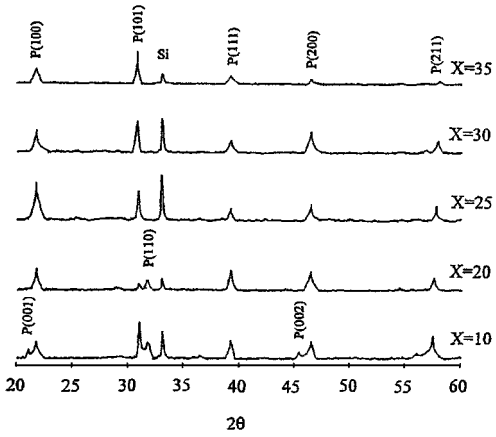

Figure 4 XRD of PLT thin films deposited at 550 °C with various La content.

precursor composition. The results clearly indicate that La contents in the thin films are lower than that in the precursor solution because of less incorporation of La. Fig. 3 also shows that the La contents in the thin films increase with La contents in the precursor solution.

The PLT thin films were transformed from tetragonal perovskite phase to the cubic perovskite phase with increasing La concentration [25]. X-ray diffraction pattern of PLT thin films deposited at 550 °C with various La content were shown in Fig. 4 which indicates that all the as-deposited films are polycrystalline perovskite. In contrast, PZT films deposited at 550 °C still contained traces of pyrochlore [24]. The result reveals that La could promote the formation of perovskite. Fig. 4 also shows that no peak splitting was observed for the La content in the precursor solution higher than 25 mol % due to the structure of PLT thin films changed from tetragonal to pseudocubic or cubic. It implied that as the La content increased the films became more cubic and less tetragonal (the c/a ratio approached unity). This

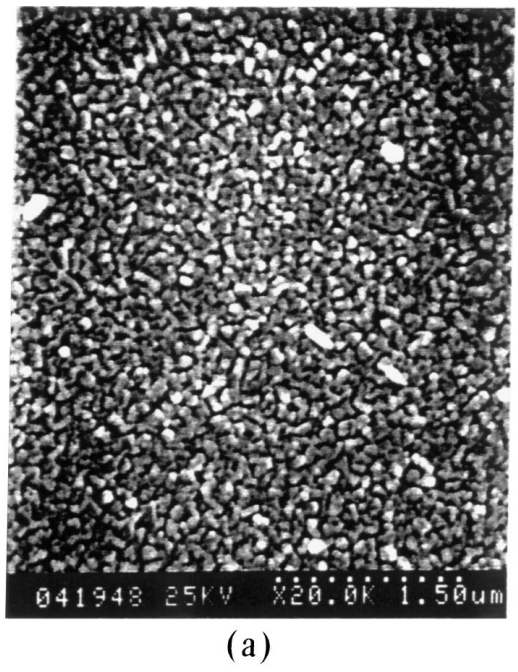

Figure 5 SEM images of three films prepared at 550 °C with different La content (a) $X = 10$, (b) $X = 20$ and (c) $X = 30$.

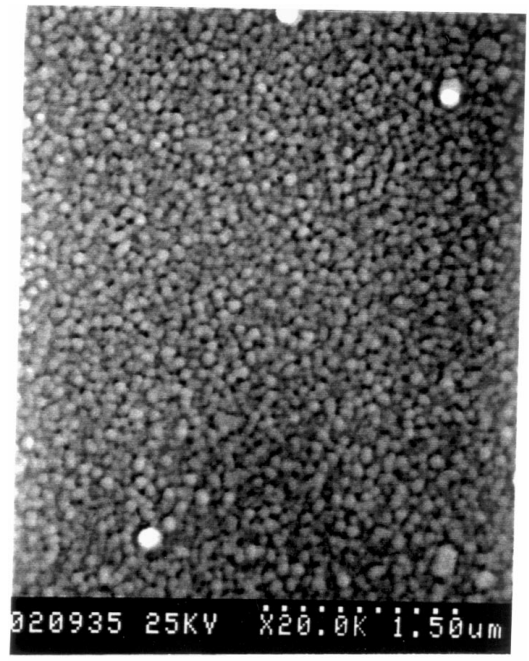

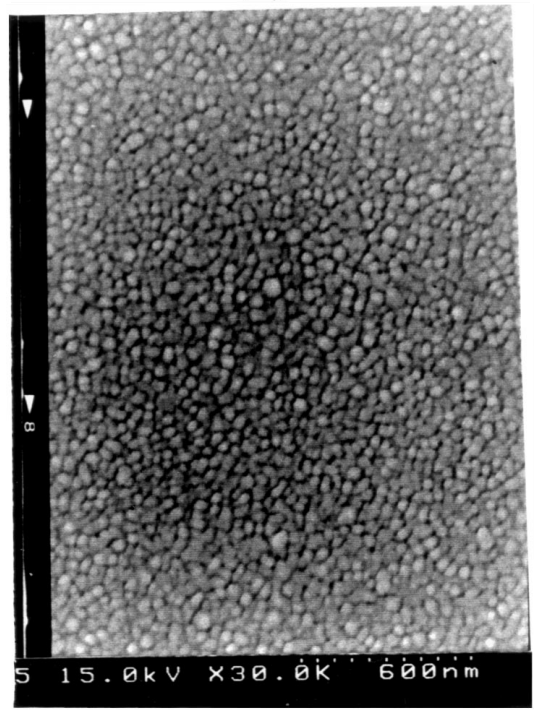

Figure 5 (*Continued*).

transformation can be also observed from the SEM micrographs of three films prepared at 550 °C with different La content, as shown in Fig. 5. The images clearly indicate that all films consist of polycrystalline grains. With lower La content, the surface shows more square. The grains of the films grown with higher La contents are finer than those grown with lower La contents. Tetragonal PLT thin films exhibite higher values of refractive index especially along the c-axis. The refractive indexes of PLT thin films deposited at 550 °C as a function of La content are plotted in Fig. 6. The indices decrease with increasing La content because of more cubic for the thin films with higher La content.

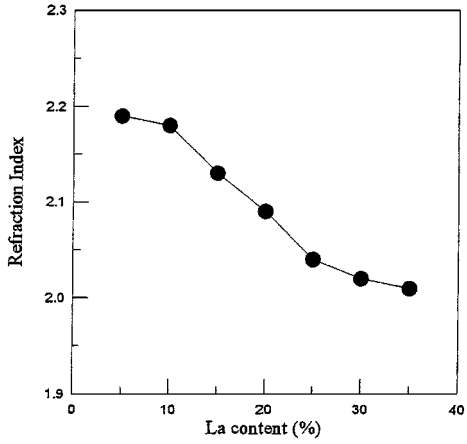

Figure 6 Dependence of refraction index on La content for films deposited at 550 °C.

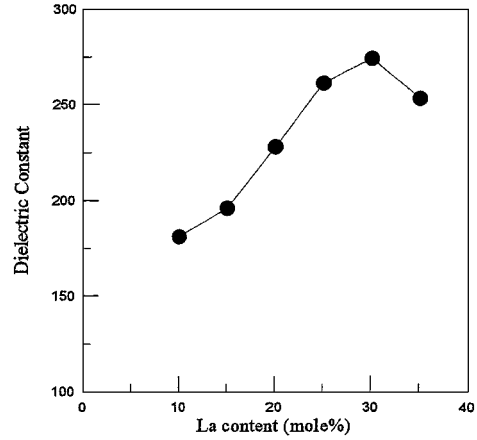

Figure 8 Dependence of dielectric constant on La content for films deposited at 550 °C.

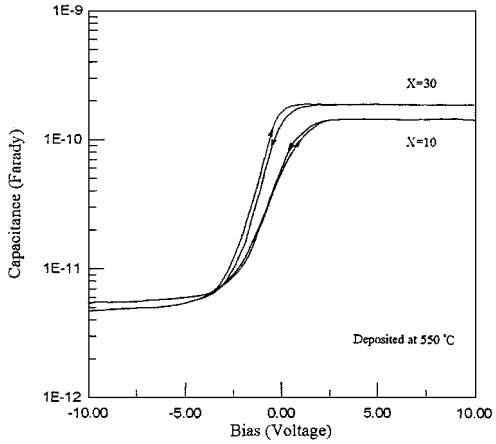

Figure 7 C-V curves measured with MIS structure at 1 Mhz.

The electrical properties of the PLT thin films grown on bare n-type (100) Si were measured with Al electrodes (2×10^{-4} cm^2 area). The structures of PLT thin films were transformed from tetragonal to cubic, resulting in the electrical property shifting from ferroelectric to paraelectric, as can be identified in Fig. 7 which shows the typical ferroelectric and non-ferroelectric C-V plots, measured from a Al/PLT/n-Si (MIS) structure at 1 MHz. One important feature in Fig. 7 is that the directions of the C-V hysteresis loops are opposite, clearly suggesting that two different kinds of charge storage mechanisms are responsible for the resultant hysteresis. The C-V hysteresis loop of film with lower La content is counterclockwise. This is due to the ferroelectric polarization. The counterclockwise direction of C-V hysteresis in ferroelectric thin film made on a n-type Si substrate agrees with the polarization concept [26]. On the other hand, the film with higher La content shows the clockwise hysteresis loop. This capacitor dielectric behaves as an ordinary insulator. It is due to charge injection at the interface rather than due to ferroelectric properties. The dielectric constant of the thin films is estimated from the maximum capacitance value in the accumulation region of the high frequency 1 MHz C-V characteristics. The effect of La content on dielectric constant for films deposited at 550 °C is plotted in Fig. 8. The dielectric constants increase from 180 to 275 with increase of the La contents from 10 to 30 mol %, while the Curie temperature (T_c) is also shifted toward room temperature [27]. These values are much smaller than those reported for MIM structure of capacitors. This can be explained by a model in which there exists a low dielectric constant layer in series with the PLT film. The origin of the low dielectric constant layer is attributed to the native SiO_2 which forms glasses in the early stage of film deposition on bare Si substrates. For films of La content in the range above 30 mol %, the dielectric constants decrease with further increase of La concentration because of particle formation and incorporation into the films, resulting in severe crystalline quality degradation. The results of I-V measurements of the Al/PLT/n-Si (MIS) structure indicate that the leakage current density is so large that the PLT thin films can not be applied to ULSI DRAMs directly. This is probably due to defect generation because of the reaction at the film-substrate interface and Pb diffusion into Si substrate.

3.2. Deposition on Pt/TiO_2/Ti/SiO_2/n-Si

From the study described above, there seems to exist intolerable disadvantages associated with the MIS structure (i.e. low dielectric constant and large leakage current density). Therefore, we deposit PLT thin films on Pt/TiO_2/Ti/SiO_2/n-Si substrates to improve the electrical properties. Fig. 9 shows the SEM micrographs of the Pt bottom electrode. The image clearly indicates that the surface shows circular grains and is more coarse than the Si substrate. Therefore, the microstructure of the deposit on the Pt electrode is not expected to be the same as that on the Si substrate.

Fig. 10 shows the X-ray diffraction patterns of PLT thin films deposited at 550 °C with various La content. They indicate that all the as-deposited films are polycrystalline perovskite and with ⟨100⟩ preferential orientation for the precursor solution with La content lower than 20 mol %. Fig. 10 also shows that no peak splitting is observed for the films deposited from the precursor solution with La concentration larger than 10 mol %. In contrast, the XRD peaks of the aforementioned PLT

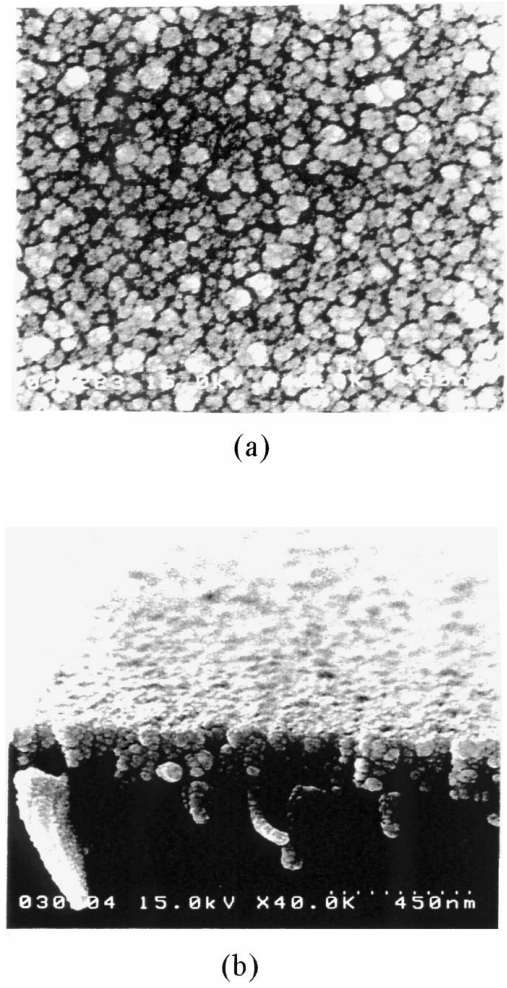

Figure 9 SEM images of Pt bottom electrode (a) plane view and (b) cross-sectional view.

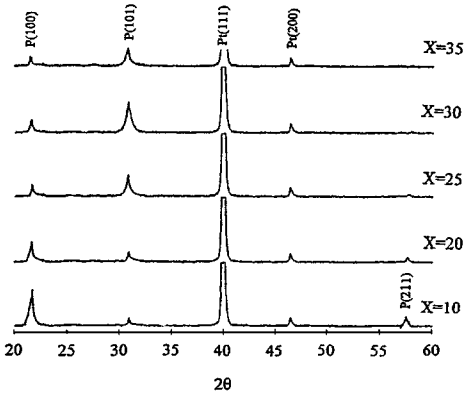

Figure 10 XRD of PLT thin films deposited on Pt bottom electrode at 550 °C with various La content.

films deposited on bare Si from the precursors with La content up to 25 mol % split. This is likely due to the influence of the surface morphology of the Pt bottom electrode.

The electrical properties of the PLT thin films grown on $Pt/TiO_2/Ti/SiO_2/n$-Si substrates are measured from the MIM samples with Pt top electrodes (2×10^{-4} cm^2 area). Fig. 11 shows the C-V curves measured from a Pt/PLT/Pt (MIM) structure at 1 MHz for the PLT thin films deposited at 550 °C with various La content. We

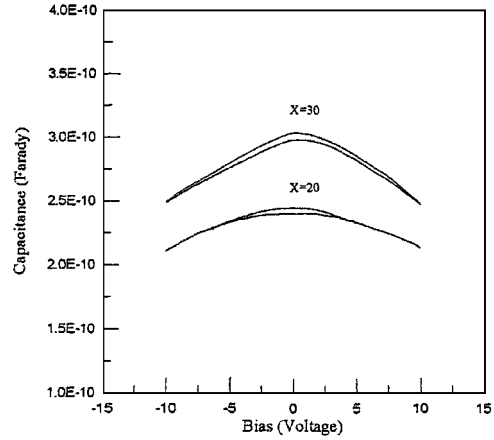

Figure 11 C-V curves measured with MIM structure at 1 Mhz.

can see from this figure that the curves do not have two peaks which are always observed from the typical ferroelectric C-V curves. The bended curves reflect the nature of paraelectric material. The C-V curves of the common dielectric thin films measured from the MIM structure shall be a horizontal line, (i.e. capacitance value is independent of the applied electric field). However, in Fig. 11 the curves bend downward at high applied electric field. The decrease in capacitance at high applied electric field can be explained by a model that a low dielectric constant layer exists in series with the PLT layer. The origin of the low dielectric constant layer can be attributed to the generation of the space-charge layer which is induced by the electrical field near the PLT film surface [28]. The data in Fig. 11 indicate that the films behave like a normal dielectric with La content larger than 20 mol %. These phenomena are also identified in Fig. 12, which is measured by using RT66A for the films deposited at 550 °C with various La content. The shape of the P-E hysteresis loop became slimmer as the La concentration increases. The hysteresis loop should be straight lines in the paraelectric state. In fact, very slim loops are observed instead of straight lines. PLT thin films are typical relaxor ferroelectrics, therefore P-E loops will not disappear over T_c immediately, because of the diffuse phase transition caused by inhomogeneities in microregions [29]. Dielectric constants as a function of La content for the PLT thin films deposited at 550 °C are shown in Fig. 13. The dielectric constants increase from 300 to 530 with increase of the La content from 10 to 30 mol % and then decrease with further increase of La content for the same reason as the aforementioned MIS structure. These values are larger than the measured values for MIS capacitors because of the films deposited on the Pt bottom electrodes can prevent the reaction at the film-substrate interface from occurring to form low permittivity glasses. On the other hand, these values are lower than those reported for bulk PLT ceramics [30], which can be attributed to the following reasons: residual porosity in the thin films, intrinsic stress [31–33], and space-charge layer [28]. The leakage current density is plotted as a function of the electric field with various La content for films deposited at 550 °C in Fig. 14. In the range of La content below 20 mol %, the leakage current density

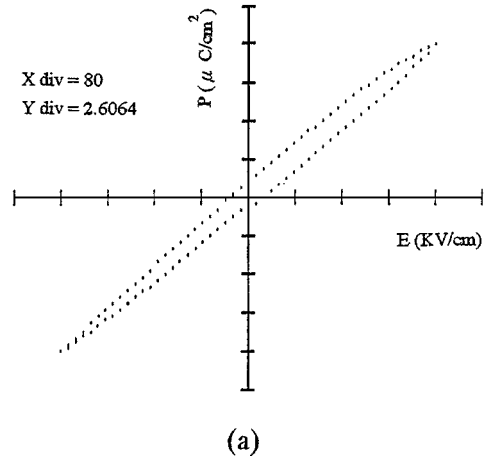

(a)

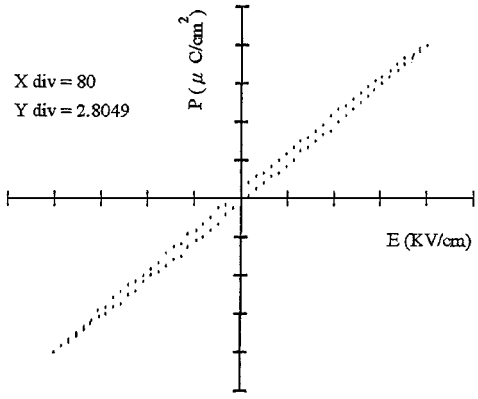

(b)

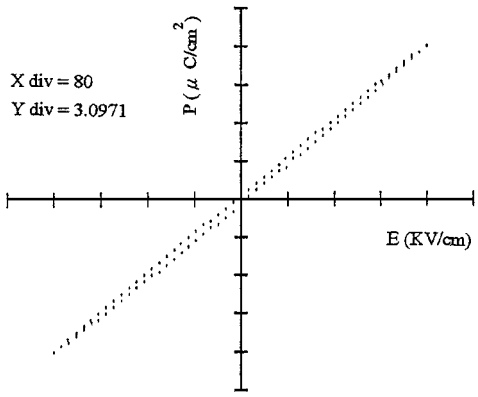

(c)

Figure 12 P-E curves of films deposited at 550 °C (a) $X = 20$, (b) $X = 25$ and (c) $X = 30$.

increases with La content at the electric field lower than 4×10^5 V/cm since La is an off-solvent dopant for Pb. However, with higher La content such as PLT(25) and PLT(30), the values of leakage current density are 6×10^{-7} A/cm^2 and 5×10^{-7} A/cm^2 at an applied electric field of 5×10^5 V/cm respectively. These values are lower than that of other films of different La contents. Fig. 14 also shows that the PLT(25) thin film exhibited the lowest leakage current at the electric field higher than 6×10^5 V/cm.

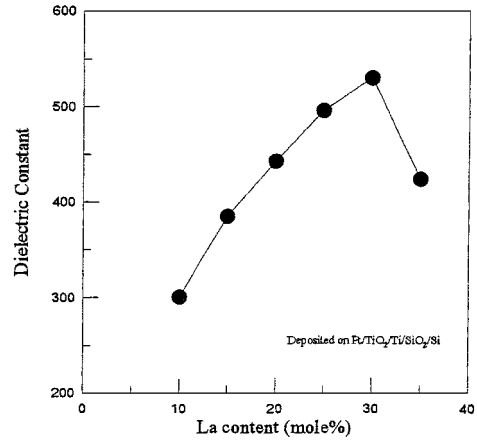

Figure 13 Dependence of dielectric constant on La content for films deposited at 550 °C.

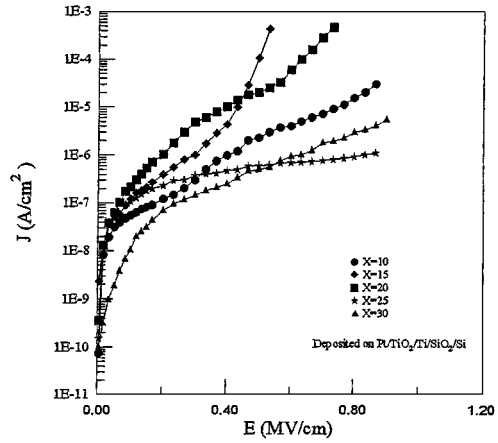

Figure 14 Leakage current density versus applied electrical field of various La content for films deposited at 550 °C.

4. Conclusions

Ultrasonic nebulized spray pyrolysis for the deposition of PLT thin films on n-type (100) Si and $Pt/TiO_2/Ti/SiO_2/(100)Si$ substrates was investigated. The main results obtained are as follows:

(1) The as-deposited low La content films are tetragonal polycrystalline perovskite which transforms to pseudocubic or cubic with increasing La content.

(2) The refractive index and grain size decrease with increasing La content.

(3) The C-V characteristics of the MIS capacitor show the clockwise hysteresis loop for the films with La content higher than 25 mol %. The dielectric constants increase from 180 to 275 with increase of the La content from 10 to 30 mol %.

(4) The results of I-V measurements of MIS structures indicate that the leakage current densities are high and can not be applied to ULSI DRAMs.

(5) The C-V curves of the MIM capacitors bend downward at high applied electric field due to generation of the space-charge layer which is induced by the electric field near the PLT film surface. The dielectric constants increase from 300 to 530 with increase of the La content from 10 to 30 mol %. These values are larger than that of the MIS capacitors.

(6) The shape of the P-E hysteresis loop becomes slimmer as La concentration increases.

(7) For the MIM structure, the leakage current densities of PLT(25) and PLT(30) thin films were 6×10^{-7} A/cm^2 and 5×10^{-7} A/cm^2 respectively at an applied electric field of 5×10^5 V/cm. The PLT(25) thin film exhibits the lowest leakage current density at electric fields higher than 6×10^5 V/cm. The leakage current densities of the MIM structures are lower than that of the MIS structures.

This work clearly demonstrates that PLT thin films can be deposited by using the ultrasonic nebulized spray pyrolysis method. The results reveal excellent electrical properties for the PLT thin films deposited on $Pt/TiO_2/Ti/SiO_2/(100)Si$ substrate and can be applied to the next generation ULSI DRAMs.

Acknowledgement

The authors gratefully acknowledge the support of the work by National Science Council of ROC (Contract # NSC86-2215-E006-007).

References

1. L. H. PARKER and A. F. TASCH, *IEEE Circuit and Devices Mag.* (Jan. 1990) 17.
2. A. F. TASCH and L. H. PARKER, *Proc. IEEE* **77** (1989) 374.
3. S. K. DEY and J. J. LEE, *IEEE Trans. Electron Devices* **39** (1992) 1607.
4. T. HASE and T. SHIOSAKI, *J. Appl. Phys.* **30** (1991) 2159.
5. M. A. KINAGA, H. FUKUDA, H. OHKUBO, T. FVKAMI and T. AOMINE, *Jpn. J. Appl. Phys.* **31** (1992) 2978.
6. K. IIJIMA, Y. TOMITA, R. TAKAYAMA and L. UEDA, *J. Appl. Phys.* **60** (1986) 361.
7. R. TAKAYAMA and Y. TOMITA, *J. Appl. Phys.* **65** (1989) 1666.
8. K. KUSHIDA and H. TAKEUCHI, *Ferroelectrics* **108** (1990) 1609.
9. K. IIJIMA, L. UEDA and K. KUGIMIYA, *Jpn. J. Appl. Phys. Lett.* **63** (1993) 2570.
10. H. HU and S. KRUPNIDHI, *Appl. Phys. Lett.* **61** (1992) 1246.
11. C. J. CHEN, E. T. WU, Y. H. XU, K. C. CHEN and J. D. MACKENZIE, *Ferroelectrics* **112** (1990) 321.
12. G. YI, Z. WU and M. SAYER, *J. Appl. Phys.* **64**(5) (1988) 1.
13. G. TEOWEE, C. D. BAERTLEIN, S. MOTAKEF, E. L. QUACKENBUSH, J. M. BOULTON and D. R. UHLMANN, *Integrated Ferroelectrics* **11** (1995) 47.
14. S. J. KANG, J. S. RYOO and Y. S. YOON, *Mat. Res. Soc. Symp. Proc.* **361** (1995) 281.
15. S. J. LEE, M. S. JANG, C. R. CHO, K. Y. KANG and S. K. HAN, *Jpn. J. Appl. Phys.* **34** (1995) 6133.
16. D. ROY, D. B. KRUPANIDHI and J. P. DOUGHERTY, *J. Appl. Phys.* **69** (1991) 7930.
17. J. S. HORWITZ, K. S. GRABOWSKI, D. B. CHRISEY and R. Z. LEUCHTER, *Appl. Phys. Lett.* **58** (1991) 2910.
18. W. REN, Y. LIU, J. QIU, L. Y. ZHANG and X. YAO, *Ferroelectrics* **152** (1994) 201.
19. Y. SAKASHITA, T. ONO and H. SEGAWA, *J. Appl. Phys.* **69**(12) (1991) 15.
20. M. OKADA, S. TAKAI, M. AMEMIYA and K. TOMINAGA, *Jpn. J. Appl. Phys. Lett.* **28** (1989) 1030.
21. Z. C. FENG, B. S. KWAK and A. ERBIL, *Mat. Res. Soc. Symp. Proc.* **361** (1995) 331.
22. D. B. BEACH and C. E. VALLET, *Mat. Res. Soc. Symp. Proc.* **415** (1996) 225.
23. J. C. VIGUIE and J. SPITZ, *J. Electrochem. Soc.* **122** (1975) 585.
24. C. S. HUANG, C. S. TAO and C. H. LEE, *J. Electrochem. Soc.* **144** (1997) 3556.
25. K. H. HARDTL, *Ferroelectrics* **12** (1976) 9.
26. SALAMA, C. T. and SICIUNAS E., *J. Vac. Sci. Technol.* **9** (1972) 91.
27. T. YAMAMOTO, H. IGARASHI and K. OKAZAKI, *J. Amer. Ceram. Soc.* **66** (1983) 363.
28. S. ROBERTS, *Phys. Rev.* **71** (1947) 890.
29. W. REN, Y. LIU, J. QIU, L. ZHANG and X. YAO, *Ferroelectrics* **152** (1994) 201.
30. D. HENNINGS and K. H. HARDTL, *Phys. Stat. Sol.* **3** (1970) 456.
31. Y. SAKASHITA, T. ONO, H. SEGAWA, K. TOMINAGA and M. OKADA, *J. Appl. Phys.* **69** (1991) 8352.
32. Y. SAKASHITA, T. ONO, H. SEGAWA, K. TOMINAGA and M. OKADA, *Ferroelectrics* **133** (1992) 79.
33. H. K. PULKER and J. MASER, *Thin Solid Films* **59** (1979) 65.

Received 23 February
and accepted 21 August 1998